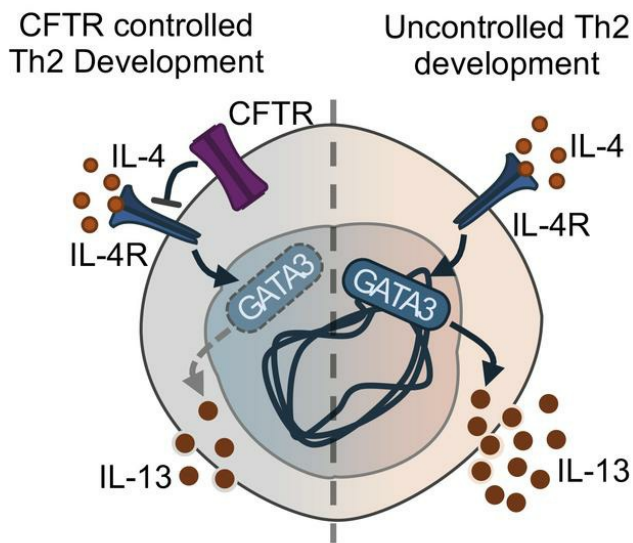# CFTR negatively reprograms Th2 cell responses and CFTR potentiation restrains allergic airway inflammation

Mark Rusznak, … , R. Stokes Peebles Jr., Daniel P. Cook

Research  In-Press Preview  Immunology  Inflammation  Pulmonology

**Graphical abstract**



**Find the latest version:**

https://jci.me/191098/pdf

# Title: CFTR negatively reprograms Th2 cell responses and CFTR potentiation restrains allergic airway inflammation

**Authors:** Mark Rusznak[1], Christopher M. Thomas[1], Jian Zhang[1], Shinji Toki[1], Weisong Zhou[1], Masako Abney[1], Danielle M. Yanda[2], Allison E. Norlander[3], Craig A. Hodges[4], Dawn C. Newcomb[1,5], Mark H. Kaplan[6], R. Stokes Peebles, Jr.[1,5,7] Daniel P. Cook[1,2,8]

**Affiliations:**

[1]Department of Internal Medicine, Vanderbilt University Medical Center; Nashville, Tennessee, USA.

[2]Department of Internal Medicine, University of Iowa; Iowa City, Iowa, USA.

[3]Department of Anatomy, Cell Biology, and Physiology, Indiana University School of Medicine; Indianapolis, Indiana, USA.

[4] Department of Genetics and Genome Sciences, Case Western Reserve University School of Medicine; Cleveland, Ohio, USA.

[5]Department of Pathology, Microbiology, and Immunology, Vanderbilt University Medical Center; Nashville, Tennessee, USA.

[6]Department of Microbiology and Immunology, Indiana University School of Medicine; Indianapolis, Indiana, USA.

[7]Tennessee Valley Healthcare System, U.S. Department of Veterans Affairs; Nashville, Tennessee, USA.

[8]Immunology Graduate Program, University of Iowa; Iowa City, Iowa, USA.

Corresponding author:     Daniel Cook
                          169 Newton Rd.
                          6312B PBDB
                          Iowa City, IA 52242
                          +1(319) 384-1107
                          daniel-p-cook@uiowa.edu

The authors have declared that no conflict of interest exists.

**ABSTRACT**

Type 2 inflammatory diseases are common in cystic fibrosis (CF) including asthma, sinusitis, and allergic bronchopulmonary aspergillosis. CD4$^+$ T helper 2 (Th2) cells promote these diseases through secretion of IL-4, IL-5, and IL-13. Whether the cystic fibrosis transmembrane conductance regulator (CFTR), the mutated protein in CF, has a direct effect on Th2 development is unknown. Using murine models of CFTR deficiency and human CD4$^+$ T cells, we show CD4$^+$ T cells expressed *Cftr* transcript and CFTR protein following activation. Loss of T cell CFTR expression increased Th2 cytokine production compared to control cells. Mice with CFTR-deficient T cells developed increased allergic airway disease to *Alternaria alternata* extract compared to control mice. Culture of CFTR-deficient Th2 cells demonstrated increased IL-4Rα expression and increased sensitivity to IL-4 with greater induction of GATA3 and IL-13 compared to control Th2 cell cultures. The CFTR potentiator ivacaftor reduced allergic inflammation and type 2 cytokine secretion in bronchoalveolar lavage of "humanized" CFTR mice following *Alternaria alternata* extract challenge and decreased Th2 development in human T cell culture. Together, these data support a direct role of CFTR in regulating T cell sensitivity to IL-4 and demonstrate a potential CFTR-specific therapeutic strategy for Th2 cell-mediated allergic disease.

**Main Text:**

**INTRODUCTION**

Cystic fibrosis (CF) is a common autosomal recessive disease caused by mutations of the gene encoding a chloride/bicarbonate channel known as the cystic fibrosis transmembrane conductance regulator (CFTR). CF is characterized by significant pulmonary morbidity and mortality as a result of recurrent inflammation and mucus accumulation in the lungs. While the main CF airway pathologic feature is severe neutrophilic inflammation, recent studies have suggested a role for type 2 inflammation, in part driven by the adaptive immune system via CD4^{+} T-helper 2 (Th2) cells activated by chronic allergen exposure (1-5). Activated Th2 effector cells produce type 2 cytokines including IL-4, IL-5, and IL-13. IL-4 and IL-13 promote the differentiation of naïve CD4^{+} cells toward Th2 development, B-cell class switching to immunoglobin E (IgE) production, and goblet cell hyperplasia. IL-5 serves as a major recruitment, differentiation, and survival factor for eosinophils. All three interleukins contribute to type 2 inflammation and have been implicated in CF immune dysregulation (2, 6-10).

Studies of persons with CF and animal models deficient of CFTR activity have shown an elevated IgE response to fungal allergens (10-13), with increased levels of IL-4 and IL-13 compared to normal CFTR function (7, 10, 13, 14). Naïve CD4^{+} T cells from *Cftr* deficient mice had elevated IL-4 production after TCR ligation (13) and increased polarization and effector function compared to CD4^{+} T cells from *Cftr*^{+/+} controls  (10, 15). In patients with CF, type 2 inflammation was a prognostic factor for *Pseudomonas* infection, and a type 2 inflammatory phenotype was correlated with increased risk of infection, pulmonary exacerbation independent of bacterial colonization, and death (3, 4, 16). In our recent studies, *Cftr*^{−/−} mice demonstrated an

3

elevated type 2 inflammatory response to the ubiquitous aeroallergen, *Alternaria alternata*, compared to *Cftr*$^{+/+}$ controls (15). In these adaptive model studies, loss of CFTR led to increased cytokine levels of IL-5 and IL-13 in the bronchoalveolar lavage fluid, greater recruitment of lymphocytes and eosinophils to the airway, and elevations in serum total IgE compared to CFTR sufficient controls. In support of a CD4$^+$ T cell specific effect, cultured Th2 cells from *Cftr*$^{-/-}$ mice in the presence of IL-33 had increased IL-13 secretion compared to similarly cultured *Cftr*$^{+/+}$ controls (15), suggesting a direct function of CFTR in inhibiting Th2 development. Despite these prior studies, whether CFTR intrinsically and negatively regulates Th2 cell function, as well as the effects of CFTR-targeted therapy in CD4$^+$ T cells remain poorly understood.

The goal of this study was to determine whether CFTR negatively regulates CD4$^+$ T cell differentiation and effector function in allergic disease and if strategies to increase CFTR function may provide therapeutic potential in airway inflammation through T cell direct and indirect mechanisms. To test this hypothesis, we aimed to (i) assess T cell specific CFTR loss in *in vitro* and *in vivo* models of allergic airway inflammation, (ii) determine the molecular pathways underlying increased CD4$^+$ T cell effector function in response to CFTR functional loss, and (iii) test for the therapeutic benefit of CFTR potentiation in Th2 mediated allergic disease.

**RESULTS**

**CFTR is expressed in CD4$^+$ T cells and induced with T cell activation**

To investigate whether mouse CD4$^+$ T cells express CFTR, we isolated RNA and performed

reverse transcriptase polymerase chain reaction (PCR). *Cftr* mRNA was present in freshly

isolated CD4$^+$ T cells from splenocytes from *Cftr*$^{+/+}$ mice, but absent in CD4$^+$ T cells from

*Cftr*$^{-/-}$ mice (**Figures 1A and S1**). CD62L$^{hi}$CD44$^{lo}$CD4$^+$ (naïve) T cells were isolated and either

processed for RNA or cultured with anti-CD3 (1µg/ml) and anti-CD28 (0.5 µg/ml) for 24 hours

(**Figure S2**). The resulting RNA was then used to perform quantitative PCR (qPCR) to

determine the relative abundance of *Cftr* transcript in *Cftr*$^{+/+}$ and *Cftr*$^{-/-}$ mouse CD4$^+$ T cells at 0

hour (naïve) and 24 hours post activation (**Figure 1B**). When normalized to naïve *Cftr*$^{+/+}$ CD4$^+$

T cells, *Cftr*$^{+/+}$ CD4$^+$ T cells activation resulted in a significant increase in *Cftr* transcript, an

effect not seen in activated *Cftr*$^{-/-}$ CD4$^+$ T cells. Immunostaining showed that CFTR primarily

localized to both surface and intracellular compartments in a subset of cultured and

activated *Cftr*$^{+/+}$ CD4$^+$ T cells at 24 hours (**Figure 1C**). CFTR was not detected in cultured CD4$^+$

T cells from *Cftr*$^{-/-}$ mice. To determine whether CFTR expression occurs in human CD4$^+$ T

cells, cell lysates from an immortalized cell line of T lymphocyte cells (Jurkat) were

immunoprecipitated with an antibody directed to the R domain of CFTR (UNC450) or isotype

(IgG$_1$) control and immunoblotted with an antibody directed to the second nucleotide binding

domain of CFTR (UNC596). Immunoblot of the immunoprecipitated Jurkat cellular lysates

revealed the presence of an approximately 170 kDa band consistent with CFTR in the CFTR

immunoprecipitated samples but not in the isotype control samples (**Figure 1D**).


To understand the temporal kinetics of *Cftr* expression following activation and/or polarization

of the CD4$^+$ T cell, we next measured relative *Cftr* transcript abundance following activation

with anti-CD3 (1µg/ml) and anti-CD28 (0.5 µg/ml) and polarization towards Th2, Th1, and Th17

cell subsets (**Figures 1E-G**), with stimulation as follows: Th2: anti-IFN-γ (10 µg/ml) and mouse IL-4 (10 ng/ml); Th1: anti-IL-4 (10 µg/ml) and mouse IL-12 (10 ng/ml); and Th17:  human TGF-β (0.5 ng/ml), mouse IL-23 (10 ng/ml), mouse IL-6 (40 ng/ml), mouse IL-1β (10 ng/ml), anti-IL-4 (10 µg/ml), and anti-IFN-γ (10 µg/ml). T regulatory cells (Tregs) were polarized and restimulated with anti-CD3 (1 µg/ml), human IL-2 (100 IU/ml), and recombinant human TGF-β (0.5 ng/ml) (**Figure 1H**). In all four subsets, a significant increase in *Cftr* transcript was noted by 18 hours, with the largest increases in Th2 and Th17 subsets. By 48 hours, *Cftr* transcript levels returned to undetectable levels in all four subsets.  Restimulation with respective activation/polarization cytokines and monoclonal antibodies (mAbs) significantly induced *Cftr* transcript to a small level in Tregs (**Figure 1H**), but there was significantly increased *Cftr* transcript in Th2 cells nearly 20 times the amount at the 18 hour timepoint (**Figure 1E**). Taken together, these results demonstrate that CFTR is expressed in CD4$^+$ T cells, *Cftr* is induced with activation, and Th2 cells display the greatest amounts of *Cftr* transcript changes with restimulation.


**CFTR negatively regulated Th2 effector function**

Given our previously published studies demonstrating increased type 2 inflammation with loss of CFTR and our data showing Th2 cells induce *Cftr* transcript following activation and polarization, we hypothesized that CFTR functions as a negative regulator of Th2 cell function. To test this hypothesis, we isolated naïve T cells from *Cftr*$^{+/+}$ and *Cftr*$^{-/-}$ mouse spleens, provided TCR ligation with anti-CD3 (1µg/ml) and anti-CD28 (0.5 µg/ml), and polarized with mouse IL-4 (10 ng/ml) and anti-IFN-γ (10 µg/ml) for 3 days prior to flow cytometry and cellular supernatant analysis (**Figure 2A**). After 3 days of culture in these conditions, *Cftr*$^{-/-}$ CD4$^+$ T

cells secreted significantly more IL-5 (**Figure 2B**) and IL-13 (**Figure 2C**) as measured in the

cellular supernatant compared to $Cftr^{+/+}$ CD4$^+$ T cells. Single-cell analysis of cultured cells by

flow cytometry revealed a larger percentage of IL-13$^+$ CD4$^+$ T cells (**Figure 2D**) and a higher

median fluorescence intensity of IL-13 in $Cftr^{-/-}$ CD4$^+$ T cells compared with $Cftr^{+/+}$ CD4$^+$ T

cells (**Figure 2E**). No differences were observed in proliferative capacity of $Cftr^{-/-}$ CD4$^+$ T cells

compared with $Cftr^{+/+}$ CD4$^+$ T cells (**Figure S3A-B**). Intracellular IL-4 was expressed in a higher

percentage, but on a per cell basis to similar amount based on MFI in $Cftr^{-/-}$ CD4$^+$ T cells

compared with $Cftr^{+/+}$ CD4$^+$ T cells (**Figure S4A-C**). Th1 and Th17 polarized $Cftr^{-/-}$ CD4$^+$ T

cells secreted similar amounts of IFN-γ and IL-17, respectively, compared to $Cftr^{+/+}$ CD4$^+$ T

cells, while Treg polarized $Cftr^{-/-}$ CD4$^+$ T cells secreted increased IL-10 compared to

$Cftr^{+/+}$ CD4$^+$ T cells (**Figure S5A-C**).


To limit the possible confounding of systemic and chronic CFTR loss towards intrinsic Th2

skewing and to test whether acute loss of CFTR would increase CD4$^+$ T cell cytokine

production, $Cftr^{+/+}$ CD4$^+$ T cells were cultured under similar Th2 polarizing conditions in the

presence of the CFTR inhibitor GlyH-101 (500 nM) or DMSO (1% v/v) control for 3 days.

Compared to DMSO treated $Cftr^{+/+}$ CD4$^+$ T cells, acute inhibition of CFTR by GlyH-101

significantly increased the amount of secreted IL-13 (**Figure 2F**). Since we observed increased

Th2 effector function in CD4$^+$ T cells absent functional CFTR in knockout and pharmacological

inhibition models, we next hypothesized that increased CFTR function reduces Th2 effector

function. To test this, we utilized the approved CFTR potentiator ivacaftor (1 μM) to increase the

open probability of CFTR channels, and the CFTR correctors elexacaftor (3 μM) and tezacaftor

(3 μM, elexacaftor-tezacaftor-ivacaftor [ETI]) to augment CFTR folding in a recently developed

"humanized CFTR" mouse model (17, 18). This mouse model which was generated in a *Cftr* null

background with a bacterial artificial chromosome transgene carrying the complete human *CFTR*

gene including its regulatory elements was critical for these experiments as the CFTR potentiator

ivacaftor is unable to potentiate mouse CFTR (19, 20). Conversely, ivacaftor is capable of

potentiating mutated and wildtype human CFTR (21). CD4$^+$ T cells isolated from mice deficient

in mouse CFTR (*Cftr*$^{-/-}$) but possessing the human *CFTR* transgene (*hCFTR*) and similar mice

possessing a mutation in the human *CFTR* gene resulting in a deletion of phenylalanine 508

(*hCFTR*$^{\Delta F508}$) were cultured in Th2 polarizing conditions with either ETI or DMSO (control).

Mutated *hCFTR*$^{\Delta F508}$ CD4$^+$ T cells had significantly increased IL-5 (**Figure 2G**) and IL-13

(**Figure 2H)** secretion in the cellular supernatant compared to *hCFTR* CD4$^+$ T cells in control

conditions. ETI significantly reduced IL-5 and IL-13 secretion in both genotypes. No differences

were observed in the proliferative capacity of ETI treated *hCFTR* CD4$^+$ T cells compared

with DMSO treated *hCFTR* CD4$^+$ T cells (**Figure S6A-B**). These results demonstrated that loss

of CFTR function increased Th2 effector function, and that conversely, augmentation of CFTR

function significantly reduced CD4$^+$ T cell secretion of type 2 cytokines.


**T cell-specific loss of CFTR increases allergic inflammation**

To test whether T cell specific loss of CFTR increases allergic inflammation to *Alternaria*

extract  (AE), we created a mouse T cell-specific *Cftr* knockout model by crossing previously

described *Cftr*$^{fl/fl}$ mice (22) to CD4$^{Cre+}$ mice (23), specifically deleting CFTR during T cell thymic

development. To test the role of CFTR in T cells during allergic inflammation,

*CD4*$^{Cre+}$*Cftr*$^{fl/fl}$ and *CD4*$^{Cre-}$*Cftr*$^{fl/fl}$ littermate mice were sensitized and challenged with either *AE*

(7.5 µg) or PBS control using an adaptive model of allergic airway inflammation (**Figure 3A**).

Extract of *Alternaria*, a ubiquitous fungal aeroallergen, was used as the airway antigen challenge as it is a common fungal sensitizing antigen in CF (24), is associated with strong bronchial provocations in CF (25), and elicits a strong type 2 airway immune response, greater in *Cftr* deficient compared to *Cftr* sufficient mice (15). To broadly assess the adaptive immune response in this model, serum total IgE was measured. IgE was significantly increased in *AE*-challenged $CD4^{Cre-}Cftr^{fl/fl}$ mice compared with PBS-challenged mice, and *AE* challenge further significantly increased IgE in $CD4^{Cre+}Cftr^{fl/fl}$ mice compared with $CD4^{Cre-}Cftr^{fl/fl}$ mice (**Figure 3B**). To assess whether these serum IgE changes correlated with type 2 inflammatory cell airway recruitment, *AE*-induced cellular inflammation was assessed in the bronchoalveolar lavage fluid (BALF, **Figure 3C-F**). BALF cell differential counts revealed marked increases in inflammation in *AE*-challenged $CD4^{Cre+}Cftr^{fl/fl}$ and $CD4^{Cre-}Cftr^{fl/fl}$ mice compared with PBS challenge, with increases in eosinophils (**Figure 3E**) and lymphocytes (**Figure 3F**). T cell specific loss of CFTR increased the overall type 2 inflammatory response, including significant elevations in recruited eosinophils and lymphocytes compared to $CD4^{Cre-}Cftr^{fl/fl}$ controls (**Figure 3E-F**). Cell type specific percentage changes were only noted in comparison of PBS and *AE*-challenged BALF, demonstrating that *AE* induced a predominately eosinophilic response in both $CD4^{Cre+}Cftr^{fl/fl}$ and $CD4^{Cre-}Cftr^{fl/fl}$ mice (**Figure S7A-D**). Consistent with these findings, loss of CFTR in CD4$^+$ T cells significantly increased IL-5 (**Figure 3G**) and IL-13 (**Figure 3H**) cytokine secretion measured in BALF of $CD4^{Cre+}Cftr^{fl/fl}$ compared to $CD4^{Cre-}Cftr^{fl/fl}$ mice. These data demonstrate that in addition to previously characterized epithelial contributions to the exaggerated type 2 immune response seen in $Cftr^{-/-}$ mice (15), the intrinsic loss of CFTR in CD4$^+$ T cells increased Th2 effector cytokine release and augmented type 2 adaptive immune responses.

**Loss of CFTR in Th2 cells increased transcripts related to the IL-4/GATA3 axis**

We next used our mouse Th2 culture model to probe Th2 transcriptional changes due to CFTR loss. Naïve CD4$^+$ T cells were isolated and stimulated with anti-CD3, anti-CD28, IL-4, and anti-IFN-γ as described above (**Figure 4A**). On day 3 (72 hours) of culture, Th2 cells from 3 distinct biological mouse donors per genotype were assessed by RNA sequencing. Principal component analysis (PCA) demonstrated dissimilarity between the *Cftr*$^{+/+}$ and *Cftr*$^{-/-}$ Th2 cells (**Figure 4B**). Using differential expression genes (DEGs) analysis, 744 genes were differentially upregulated and 892 genes were downregulated in *Cftr*$^{-/-}$ Th2 cells compared to *Cftr*$^{+/+}$ Th2 cells (**Figure 4C, Table S2-3**). Supportive of a drive to transcribe *Cftr* mRNA in CD4$^+$ T cells, increased levels of *Cftr* transcript were observed in *Cftr*$^{-/-}$ samples, as the model is an in-frame elimination of exon 11 and capable of producing non-functional alternative mRNA (26). Functional annotation using gene set enrichment analysis (GSEA) showed that upregulation of Th2 specific pathways including those related to asthma, IL-4/IL-17 signaling, and cytokine-cytokine receptor interactions (**Figure 4D, Table S3**). A collection of T cell and Th2 related gene signatures was generated using the Th2 Cell gene set from Harmonizome multi-omics data integration platform (Ma'ayan Laboratory of Computational Systems Biology, (27)) including genes for surface markers (**Figure 4E**), cytokines (**Figure 4F**), transcription factors (**Figure 4G**), and pan markers (**Figure 4H**). Several regulators of canonical Th2 programming were increased by loss of CFTR in Th2 cells including *Il4ra*, *Il4*, *Il13*, and *Gata3*. Additional transcripts related to activation and or exhaustion were dysregulated in *Cftr*$^{-/-}$ Th2 cells compared to *Cftr*$^{+/+}$ Th2 cells including *Ccr8*, *Bcl6*, *Batf*, *Klf2*, *Myb*, *Trfrsf4* (encodes OX40), *Ctla4*, *Btla*, *Tnfrsf9* (encodes 4-1BB). Gene concept networking revealed some of the most enriched nodal terms as JAK/STAT signaling, cytokine receptor signaling, and asthma gene sets (**Figure S8A**). These three pathways

demonstrated substantial overlap in a gene concept network, further supporting the role of CFTR in modifying type 2 inflammatory signaling. Hierarchical clustering of the 30 most enriched GO:BP terms showed alterations in anion transport, fatty acid metabolic processes, amide transport, and non-coding RNA metabolic processes (**Figure S8B**). These broad categories of transcriptomic changes highlight the profound effect of CFTR loss on Th2 cells beyond canonical inflammatory pathways. Taken together, these data demonstrate that the loss of CFTR during activation and Th2 polarization fundamentally altered the Th2 transcriptome with specific skewing towards increased transcription of the IL-4/GATA3/IL-13 signaling axis.

**Loss of CFTR increased CD4$^+$ T cell sensitivity to IL-4**

Given increased secreted Th2 cell cytokines and enrichment of IL-4 signaling specific transcripts in $Cftr^{-/-}$ Th2 cells compared to $Cftr^{+/+}$ Th2 cells, we next tested the hypothesis that loss of CFTR results in augmented IL-4 signaling in CD4$^+$ T cells. To test this hypothesis, we isolated naïve CD4$^+$ T cells from splenocytes of $Cftr^{+/+}$ and $Cftr^{-/-}$ mice, cultured the cells in Th2 polarizing conditions, and harvested the resulting Th2 cells at 72 hours for analytical flow cytometry (**Figure 5A**). Loss of CFTR in Th2 cells increased expression of the alpha subunit of the interleukin 4 transmembrane receptor (IL-4Rα, **Figure 5B-C**) and upregulated expression of the downstream transcription factor target, GATA3 (**Figure 5D-E**). Since IL-4 signaling induces GATA3 expression in CD4$^+$ T cells (28), we next cultured naïve CD4$^+$ T cells with increasing doses of IL-4 (0-40 ng/ml) for 72 hours. $Cftr^{-/-}$ Th2 cells had a greater percentage of GATA3$^+$CD4$^+$ T cells at 72 hours at lower doses of IL-4 compared to $Cftr^{+/+}$ CD4$^+$ T cells (**Figure 5F**). IL-4-induced GATA3 expression (**Figure 5G**, $p<0.0001$) and secreted IL-13 in cellular supernatant (**Figure 5H**, $p< 0.0001$) was significantly increased in $Cftr^{-/-}$ CD4$^+$ T cells

compared to $Cftr^{+/+}$ CD4$^+$ T cells via four-parameter sigmoidal curve fit analyses, defined by a decreased EC$_{50}$ (1.86 ng/ml [1.42-2.87] in $Cftr^{-/-}$ CD4$^+$ T cells vs 5.316 ng/ml [3.40 – 10.86] in $Cftr^{+/+}$ CD4$^+$ T cells for secreted IL-13 comparison). No differences in IL-4Rα expression between were seen in the first ten hours $Cftr^{+/+}$ and $Cftr^{-/-}$ CD4$^+$ T cells within the first 10 hours of activation (**Figure S9A-G**). These data demonstrate that CFTR negatively regulated GATA3 expression, in part through decreased IL-4 sensitivity of CD4$^+$ T cells.

**Increased CFTR function decreased Th2 mediated allergic inflammation in a humanized CFTR mouse model**

Given our prior work demonstrating decreased human epithelial type 2 alarmin release with CFTR modulator treatment (15) and data demonstrating CFTR modulator mediated decreased Th2 effector function in mouse *hCFTR* CD4$^+$ T cells (**Figure 2G-H**), we next hypothesized that treatment with the CFTR potentiator ivacaftor reduces allergic inflammation to *AE* in *hCFTR* mice. To test whether increased CFTR function can attenuate allergic inflammation, mice expressing either mouse *Cftr* or *hCFTR* were sensitized and challenged with *AE* (7.5 μg) using the adaptive model of allergic airway inflammation and given either once daily intraperitoneal ivacaftor (10 mg/kg) or vehicle control (DMSO 5% v/v) leading up to and during sensitization and challenge (**Figure 6A**). Using IgE levels to broadly assess the adaptive immune response, we observed a significant decrease in serum total IgE amounts in ivacaftor treated *hCFTR* mice compared to vehicle control treated *hCFTR* mice (**Figure 6B**). The effect of ivacaftor treatment on *AE*-induced cellular inflammation was assessed in the BALF (**Figure 6C-F**). BALF cell differential counts revealed significantly less recruitment of macrophages (**Figure 6C**), neutrophils (**Figure 6D**), eosinophils (**Figure 6E**) and lymphocytes (**Figure 6F**) in ivacaftor

treated compared vehicle treated *hCFTR* mice. No BALF cell type specific percentage changes were noted in comparison of genotype or treatment group, indicating the primary effect of ivacaftor was diminishing the magnitude of the type 2 response (**Figure S10A-D**). Consistent with these findings, ivacaftor treatment in *hCFTR* mice significantly decreased IL-5 (**Figure 6G**) and IL-13 (**Figure 6H**) cytokine secretion measured in BALF compared to vehicle control treated mice. Importantly, no differences were noted between ivacaftor and vehicle-treated mice expressing mouse *Cftr* (*Cftr*$^{+/+}$), demonstrating ivacaftor's specificity for human CFTR (**Figure S11A-G**). These data demonstrate that *in vivo* ivacaftor treatment reduced type 2 airway inflammation to *AE*, requiring human CFTR expression to mediate the therapeutic effect.

**Increased CFTR function decreases GATA3 and IL-13 expression in human Th2 cells**

To assess whether the findings of decreased type 2 immunity with CFTR potentiation in the mouse model translate to T cell mediated inflammation in humans, naïve CD4$^+$ T cells were isolated from healthy human PBMCs and cultured in Th2 polarizing conditions for 7 days in the presence of ivacaftor or DMSO control (**Figure 7A**). The percent of viable cells was similar at 7 days between DMSO and ivacaftor treated CD4$^+$ T cells (**Figure 7B**). To test the hypothesis that CFTR potentiation decreases Th2 effector function, cultured cells were processed for analytical flow cytometry and secreted cytokine analysis (**Figure S12**). CFTR potentiation with ivacaftor in Th2 cells led to significantly decreased expression of GATA3 (**Figure 7C-D**) and intracellular IL-13 compared to DMSO control treated cells (**Figure 7E-F**). Consistent with these findings, secreted IL-13 measured in the cultured cellular supernatants was significantly decreased in ivacaftor treated CD4$^+$ T cells compared to DMSO treated cells (**Figure 7G**). Taken together,

these data demonstrate that CFTR modulation decreased Th2 effector function and suggest that targeting CFTR may represent an adjunct to current therapies in allergic disease.

**DISCUSSION**

Clinically, individuals with CF have increased rates of type 2 immune diseases including asthma, allergic rhinitis, and allergic bronchopulmonary aspergillosis (ABPA) (3, 29). Collectively these diseases represent hyperinflammatory responses defined by increased levels of IL-4, IL-13, and IgE (30-32). Prior studies have demonstrated a skewing of CF CD4^{+} T cells towards Th2 responses (8, 13, 15, 16, 33). However, the mechanisms pertaining to CFTR expression in CD4^{+} T cells and determinants for increased effector phenotypes are not well characterized. Here, we used mouse cellular and *in vivo* models deficient in CFTR, which lack any spontaneous airway infection, to study the effect of CFTR in Th2 effector function and the role of CD4^{+} T cell specific CFTR in type 2 adaptive immunity. Our results show that CFTR expression is temporally associated with CD4^{+} T cell activation and that CFTR negatively regulates Th2 effector function, in part through negative regulation of the IL-4/GATA3 axis. These results are further supported by increased type 2 inflammation to *AE* sensitization and challenge in a mouse model of CD4^{+} T cell specific loss of CFTR compared to CFTR sufficient controls.  Importantly, we report that pharmacologic potentiation of CFTR with the FDA approved compound ivacaftor is associated with decreased *AE*-induced allergic inflammation in a humanized CFTR mouse model and decreased GATA3 and IL-13 expression in human CD4^{+} T cells.

Here we build on previous studies that have shown CFTR to be expressed in CD4^{+} T cells (34-36). Consistent with our findings of CFTR expression in an immortalized CD4^{+} lymphocyte cell

line (Jurkat), early studies of cystic fibrosis demonstrated evidence of a functional cAMP-regulated chloride channel consistent with CFTR in the same cells (37). To our knowledge these early studies in CD4$^+$ T cells were the first to show non-epithelial cell CFTR expression and highlight the early recognition of CFTR intrinsic effects in CD4$^+$ T cells. Despite early identification of functional CFTR expression in lymphocytes, our understanding of the contributions of CFTR to CD4$^+$ Th2 effector function remain limited. CFTR has previously been proposed to mediate calcium flux across the T-cell plasma membrane within seconds of TCR activation, thereby regulating calcium–sensitive gene expression pathways (10). In the present studies, no *Cftr* transcript or CFTR protein was observed in the naïve T cell and was only present hours following TCR ligation. Therefore, the augmented calcium flux in CFTR deficient T cells seen in the prior studies cannot be explained by our studies and likely reflect differences in the CF model. Importantly, the prior studies used mice harboring a misfolded ΔF508 mutation of CFTR which is known to have residual functional activity yet is improperly retained in the endoplasmic reticulum and Golgi networks (38, 39), resulting in endoplasmic reticulum condensation and clustering of large-conductance cation channels. While disease relevant, these prior observations may reflect changes specific to improper CFTR localization and/or activity as opposed to the intrinsic effect of normal CFTR. Conserved in both the prior and current studies is augmented Th2 effector cytokine production in the setting of abnormal or absent CFTR (10, 13).

How might loss of CFTR contribute to the augmented Th2 response seen in our model? *Cftr*$^{-/-}$ CD4$^+$ T cells have increased Th2 effector function compared to *Cftr*$^{+/+}$ controls. No detectable *Cftr* transcript or protein was noted in naïve primary cell cultures suggesting that the major effect

of CFTR during polarization occurs hours after TCR stimulation following required transcription, translation, and trafficking of the CFTR protein. Despite having similar initial surface levels of the cytokine receptor for IL-4 (IL-4R), $Cftr^{-/-}$ CD4$^+$ T cells demonstrated increased sensitivity to IL-4, with increased GATA3 expression compared to $Cftr^{+/+}$ CD4$^+$ T cells by 72 hours. Taken together, we hypothesize that CFTR could be a target of GATA3 transcription factor activity which then acts as a feedback inhibitor against stable Th2 commitment. Indeed, within the CFTR promoter exists a putative GATA3 binding motif at site -607bp respective to the CFTR transcription start site. Further studies will be required to integrate whether GATA3 has transcriptional activity on the *Cftr* promoter. CFTR expression may subsequently modify IL-4R signaling during polarization through direct ion dysregulation via chloride and/or bicarbonate movement, via CFTR's direct protein-protein interactions with downstream signaling proteins important for IL-4 signaling such as PTEN-PI3K, or intracellular fluid homeostasis. More investigations are needed to clarify the exact mechanism of CFTR's regulation of Th2 commitment and whether there is an effect of CFTR mutational class on Th2 effector function. Together, the prior and current studies suggest that multiple mechanisms of CD4$^+$ T cell dysfunction may exist in CF disease, including contributions from the lack of CFTR and localization of CFTR.

A CFTR/IL-4R signaling axis has been implicated in other cell types responsive to IL-4. Recent studies have noted a hyper-responsiveness to IL-4 in CFTR deficient compared to CFTR sufficient B cells (8), with increased expression of BAFF, CXCR4, and IL-6 in IL-4 treated $Cftr^{-/-}$ B cells compared to $Cftr^{+/+}$ B cells (40). Equally interesting is the observation that IL-4 can induce *CFTR* expression and upregulate cAMP-dependent current in human epithelial

models (41). Taken together, these observations support our hypothesis that IL-4R signaling may induce a possible CFTR mediated "Th2 braking mechanism" while simultaneously driving canonical Th2 effector function. Further studies aimed at understanding this potential "rheostat" mechanism involving CFTR function and IL-4/GATA3 regulation will be important.

The ability of CFTR to suppress Th2 responses arising from allergy, both through epithelial-derived cytokines and Th2 cell function, provides a unique opportunity to therapeutically target a novel multicellular immunomodulatory pathway. Recently, CFTR modulators designed to improve channel function in persons with different CFTR mutations has revolutionized the clinical treatment of CF (42). CFTR potentiators such as ivacaftor increase the open probability of CFTR channels with a gating mutation, and can also increase wild type CFTR function (43, 44). We show that the CFTR potentiator ivacaftor in a mouse model of allergic disease significantly reduced allergic inflammation through reductions in recruited eosinophils and lymphocytes, as well as production of IgE compared to vehicle treated mice. Together with our prior findings demonstrating that CFTR modulation reduces epithelial release of the potent type 2 cytokine IL-33 and our present studies showing significant GATA3 and IL-13 reductions in human Th2 cells treated with ivacaftor compared to DMSO controls, CFTR modulation has the potential to broadly target allergic disease. Indeed, we and others have shown that individuals with CF have significant reductions in type 2 biomarkers after initiation of CFTR modulator therapy (3, 45). Whether these reductions in type 2 biomarkers could extend to a non-CF population and whether CFTR function can modify Th2 effector function in previously committed Th2 cells remains unstudied. CFTR targeting compounds may serve as potential

adjuvants to current allergy therapies by mechanistically targeting nonredundant pathways in allergic disease.

Our studies have both advantages and limitations. Advantages include: 1) We used comparative methodologies highlighting a conserved effect of CFTR on Th2 effector function in both humans and mice. *2*) Cre recombinase driven deletion of T cell specific CFTR in mice provided a powerful approach to assess $CD4^+$ T cell CFTR function in allergy, a method that would be more challenging in larger animal CF models. *3*) We took advantage of the lack of spontaneous lung disease in mice to determine the primary effect of allergen challenge on Th2 driven inflammation. *4*) Using recently a recently developed humanized CFTR mouse model, we demonstrated an *in vivo* ivacaftor mediated decrease in allergy through reductions in type 2 cytokines (IL-5 and IL-13) and total serum IgE. Limitations include: 1) We cannot exclude the possibility of CFTR effects on other cell types of the innate and adaptive immune system in our allergy model. CFTR expression and function has been implicated in other relevant inflammatory cell types including macrophages, B cells, and neutrophils (40, 46-50). We utilized *AE* as a potent stimulus of eosinophilic and lymphocytic inflammation, but other common aeroallergens such as host dust might may have differential effects on airway allergy in CF based on the resultant cellular inflammation. The ability of CFTR targeting therapies to alter heterogenous cell populations may be advantageous, but future studies will be required to understand how CFTR modulating therapy affects other types of inflammation. 2) We did not assess a role for other T cell subsets including Th1 and Th17 cells in this model. Although we focus primarily on the direct effects of Th2 mediated inflammation, previous studies demonstrated a Treg functional deficiency in both CF human and $Cftr^{-/-}$ mouse models (51), and

our time course analysis of CFTR expression did reveal a significant, but relative to Th2 cells, small induction of *Cftr* mRNA in Tregs. It may be possible that T cell differentiation is broadly altered by CFTR loss and further studies will be required to understand CFTR contributions to the differentiation and effector function of other T cell subsets. 3) We performed *in vitro* polarization of naïve CD4$^+$ cells to limit non-CD4$^+$ T cell contributions to the polarized Th2 cell; however, we cannot exclude that naïve CD4$^+$ T cells may be inherently reprogrammed making them more sensitive to Th2 polarizing conditions. Indeed, prior studies have found that TCR ligation alone in naïve CF CD4$^+$ T cells results in increased Th2 skewing compared to non-CF controls (13). Assessing the acute changes between CD4$^+$ T cell naivety and activation serve as attractive areas of further study to better understand not only the contributions of CFTR to Th2 effector identity but also whether CFTR targeting therapies are most viable as a preventative or relief therapy in allergic disease.

In summary, our findings demonstrate that CD4$^+$ T cells expressed CFTR following stimulation and CD4$^+$ T cell loss of CFTR significantly increased Th2 effector function *in vitro* and augmented *in vivo* allergic inflammation to *AE*. Further, we demonstrated that CFTR functions as a negative regulator of Th2 effector function, in part, by reducing the IL-4/GATA3 signaling axis. The recently approved CFTR potentiator, ivacaftor, decreased inflammation in an *in vivo* mouse allergy model and reduced GATA3 expression and effector function in *in vitro* polarized human Th2 cells. The CFTR modulator drug class may provide pharmacological approaches to managing common and persistent type 2 inflammation in CF via epithelial and CD4$^+$ T cell mechanisms, while more broadly representing a new class of therapies to be repurposed for allergic disease.

## MATERIALS AND METHODS

For additional information, see the Methods and Materials section in the online supplement.

### Sex as a biological variable

Our study examined the effect of CFTR deficiency in female mice because female animals exhibited heightened type 2 inflammation and less variability in phenotype compared to male mice. Our CFTR potentiation studies in humanized CFTR mice and human T cells, examined both male and female animals/humans, and similar findings are reported for both sexes.

### Study design

The objective of this study was 1) to determine the role of CFTR in Th2 cell function and Th2 cell-mediated allergic inflammation, 2) elucidate the underlying molecular Th2 cell signaling mechanisms, and 3) to test the therapeutic potential of a clinically approved CFTR potentiator in allergic disease. Experimental approaches comprise *in vitro* cellular studies in human and mouse CD4$^+$ T cells, next generation bulk RNA sequencing of mouse Th2 cells, and *in vivo* allergen studies in mice. Two lines of *in vivo* experimentation designed to elicit adaptive type 2 inflammation were performed, 1) PBS or *AE*-challenged $CD4^{Cre+}Cftr^{fl/fl}$ or $CD4^{Cre-}Cftr^{fl/fl}$ mice, and 2) *AE*-challenged mouse *Cftr* or *hCFTR* expressing mice treated with vehicle control or the CFTR potentiator ivacaftor. For *in vitro* experimentation, naïve $Cftr^{+/+}$ and $Cftr^{-/-}$ mouse CD4$^+$ T cells, and naïve *hCFTR* and $hCFTR^{\Delta F508}$ mouse CD4$^+$ T cells were isolated from mouse splenocytes and cultured in Th2 polarizing conditions, a subset of which were treated with

pharmacological inhibitors of activators of CFTR. Human naïve CD4$^+$ T cells were isolated from PBMCs, cultured in Th2 polarizing conditions, and treated with either DMSO control or ivacaftor. For RNA sequencing studies, *in vitro* polarized *Cftr$^{+/+}$* and *Cftr$^{−/−}$* Th2 cells were submitted for analysis.


**Animals**

For *in vitro* studies, *Cftr$^{tm1\ Unc}$*Tg(FABPCFTR)1Jaw/J mice were obtained from The Jackson Laboratory (stock no: 002364). These mice are knockouts for the mouse *Cftr* gene (*Cftr$^{−/−}$*) but express human CFTR in the gut under control of the FABP1 (fatty acid binding protein1) promoter, which prevents acute intestinal obstruction. For *in vivo* studies requiring T cell specific deletion of CFTR, adult female *CD4$^{Cre+}$Cftr$^{fl/fl}$* or their corresponding *CD4$^{Cre−}$Cftr$^{fl/fl}$* littermates were used for experiments. For *in vivo* CFTR potentiation studies, adult male and female mice deficient in mouse CFTR (*Cftr$^{−/−}$*) but possessing a human *CFTR* transgene (*hCFTR*) or same-strain (C57BL/6J) housed *Cftr$^{+/+}$* controls lacking the human *CFTR* transgene, were used. Additionally, mice possessing a mutation in the human *CFTR* gene resulting in a deletion of phenylalanine 508 (*hCFTR$^{\Delta F508}$*) and *hCFTR* mice were used for *in vitro* experiments (17, 18). All animals were maintained under specific pathogen–free conditions and 12-hour light-dark cycles with free access to food and water. The number of experimental replicates is indicated in the figure legends.


**CD4$^+$ T cell culture**

CD4$^+$ T cells were purified from the splenic cells of *Cftr*$^{+/+}$ and *Cftr*$^{-/-}$ littermate mice by either a mouse pan CD4$^+$ T cell isolation kit (19852, STEMCELL Technologies) or mouse naive CD4$^+$ T cell isolation kit (19765, STEMCELL Technologies, **Figure S2**). The purified pan CD4$^+$ or CD62L$^{hi}$CD44$^{lo}$ CD4$^+$ T cells were resuspended at $1 \times 10^6$ cells/ml in RPMI 1640 medium (Mediatech, Herndon, VA) supplemented with 10% FBS (HyClone, Logan, UT), 4 mM of l-glutamine, 1 mM of sodium pyruvate, 55 µM of 2-ME, 10 6 mM of HEPES, 100 U/ml penicillin, and 100 µg/ml streptomycin. The cells were stimulated with plate-bound anti-CD3 (1 µg/ml) and anti-CD28 (1 µg/ml; BD Biosciences, San Diego, CA) in 24-well flat-bottom plates for initial TCR ligation studies. For polarization and time course studies, naïve T cells were provided stimulation as follows: Th2: anti-IFN-γ (10 µg/ml) and mouse IL-4 (10 ng/ml); Th1: anti-IL-4 (10 µg/ml) and mouse IL-12 (10 ng/ml); and Th17: human TGF-β (0.5 ng/ml), mouse IL-23 (10 ng/ml), mouse IL-6 (40 ng/ml), mouse IL-1b (10 ng/ml), anti-IL-4 (10 µg/ml), and anti-IFN-γ (10 µg/ml). T regulatory cells (Tregs) were polarized and restimulated with anti-CD3 (1 µg/ml), human IL-2 (100 IU/ml), and recombinant human TGF-β (0.5 ng/ml) and for Th2 polarization also stimulated with mouse IL-4 (10 ng/ml). For time course studies, cells were harvested for cellular RNA at times 0, 6, 18, and 72 hours post polarization as well as 6 hours post restimulation (78 hour) with TCR ligation and subset specific stimulation as above. For Th2 specific studies, after 3 days, the culture supernatant was harvested for multiple cytokine ELISA assays. Cellular RNA was collected for RNAseq as described below. For humanized CFTR CD4$^+$ T cell studies, cells from *hCFTR*$^{ΔF508}$ and *hCFTR* mice were isolated and polarized in Th2 conditions as above, in the presence of the CFTR potentiator ivacaftor (1µM), and the CFTR correctors elexacaftor (3µM) and tezacaftor (3µM, elexacaftor-tezacaftor-ivacaftor [ETI]) or DMSO control (%5 v/v).

For human cell CD4$^+$ T cell studies, human PBMCs were prepared from whole blood of healthy donors by Ficoll density gradient centrifugation using Lymphoprep density gradient medium (StemCell Technologies) and SepMate-50 tubes (StemCell Technologies). For the purification of human naive CD4$^+$ T cells, an EasySep human naive CD4$^+$ T cell isolation kit II (StemCell Technologies) was used. The purification procedures were carried out according to the supplier's instructions. For expansion, cells were cultivated in ImmunoCult-XF T Cell Expansion Medium (StemCell Technologies). The media was supplemented with ImmunoCult Human Th2 Differentiation Supplement (containing recombinant human IL-4 and mouse anti-human IFN-γ, StemCell Technologies) and 100 IU/mL IL-2 (NIH). T cells were activated by 25 µL/mL ImmunoCult Human CD3/CD28/CD2 T Cell Activator reagent at a cell density of $1 \times 10^6$ cells/mL (StemCell Technologies). After 7 days, cells were collected for analytical flow cytometry and the culture supernatant was harvested for multiple cytokine ELISA assays.

**RNA sequencing**

Cellular RNA was isolated from cultured mouse *Cftr*$^{+/+}$ and *Cftr*$^{-/-}$ Th2 cells representing three biologic replicates for each genotype. Genomic DNA was digested using DNase I (Qiagen). RNA samples were then quantified using fluorimetry (Qubit 2.0 fluorometer; Life Technologies), and RNA quality was assessed using an Agilent BioAnalyzer 2100 (Agilent Technologies). Only samples with RNA integrity numbers >8.0 were used. Library preparation and sequencing were conducted in the Vanderbilt Technologies for Advanced Genomics (VANTAGE) core facility. Briefly, an Illumina Ribo-Zero Plus rRNA Depletion kit was used to isolate rRNA-depleted RNA. The samples were then reverse transcribed to create cDNA. The

cDNA was fragmented, blunt-ended, and ligated to indexed adaptors. Following quantification of the cDNA generated for the library, the samples were clustered and loaded equally over two lanes on an Illumina NovaSeq6000 Sequencing system (Illumina Inc.), which generated on average >45 million paired reads of 150 bp. For analysis, raw data were aligned and counted to the GRCm38 reference genome by the Dragen workflow provided by VANTAGE. For downstream analysis, all samples were normalized by Trimmed Mean of M-values (TMM) with DESeq2 package. PCA plot was generated from these normalized values, and $\log_2$ fold change values were calculated, and its output was used for volcano plot construction and gene set enrichment for KEGG pathway and Harmonizome geneset analysis (Ma'ayan Laboratory). Significant differential expression was determined in genes with FDR-adjusted p value < 0.01 and fold change ± 1.5. Additional gene set enrichment analysis (GSEA) was performed with the clusterProfiler R package (52) on a ranked list of differentially expressed genes sorted by log2(fold change) using Gene Ontology: Biological Processes (GO:BP) and KEGG curated gene sets. Gene sets with an adjusted p value <0.05 were considered significant. The Gene-Concept Network was generated from highly enriched KEGG gene sets of interest relating to cell signaling (KEGG_ASTHMA, KEGG_JAK_STAT_SIGNALING_PATHWAY, and KEGG_CYTOKINE_CYTOKINE_RECEPTOR_INTERACTION). Hierarchical clustering of the 30 most enriched GO:BP terms by Jaccard's similarity index was performed with clusterProfiler, DOSE, and enrichplot R packages. Terms were grouped into 4 clusters with 1 label term per cluster. Both plots were visualized with ggplot2.

**Alternaria-extract challenge in mice**

Mice were anesthetized under continuous delivery of isoflurane and oxygen into a chamber placed within a sterile hood. For the adaptive model, from day 0 to day 2, either 7.5 µg (protein amount) of *AE* in 80 µl of PBS or 80 µl of PBS as vehicle were administered intranasally to anesthetized mice. *AE* (7.5 µg protein amount) in 80 µl of PBS or 80 µl of PBS intranasal challenge occurred on days 15 and 16. For ivacaftor treatment experiments, *AE*-challenged mice from day -3 to 2 and day 12 to 16, either once daily ivacaftor (10 mg/kg) or vehicle control (5% DMSO v/v) was intraperitoneally administered. Whole lungs and BALF were harvested on day 17, 24 hours after the last challenge.

**Cytokine and IgE ELISAs**

Murine IL-5, mouse IL-13, and mouse IgE, was assayed using Quantikine ELISA kits following manufacturer's instructions (R&D Systems).

**Flow cytometry**

*In vitro* polarized mouse $Cftr^{+/+}$ and $Cftr^{-/-}$ Th2 cells (day 3 of culture) and human Th2 cells (day 7 of culture) were incubated in the presence of 1 µl GoliPlug (ND) for 4 hours. Cells were then resuspended in a buffer containing 2% FBS, and 2 mM EDTA (Life Technologies) in PBS then incubated with fixable Aqua dead cell stain (Invitrogen L34957) before staining with fluorophore-conjugated antibodies. Foxp3/Transcription factor Staining kit (00-5523-00, Thermo Fisher) was used to stain GATA3 and other intracellular proteins according to the manufacturing protocol. Murine cells were stained with antibodies against the following molecules (clone, conjugate; source): CD4 (GK1.5, BUV395, BD), CD3 (145-2C11, APC-Cy7, BD), CD45 (30-

F11, BB700, BD), CD124 (Astra-1, AF488, Invitrogen), IL-4 (11B11, BV650, BD), IL-13 (eBio13A, PerCP-ef710, Invitrogen), GATA3 (TWAJ, eFlour 660, Invitrogen). Human cells were stained with antibodies against the following molecules: CD4 (RPA-T4, Super Bright 780, Invitrogen), GATA3 (TWAJ, eFlour 660, Invitrogen), IL-13 (85BRD, Alexa Flour 647, Invitrogen). Data were acquired on a BD LSRFortessa SORP flow cytometer (Becton Dickinson) or Cytek Aura spectral flow cytometer (Cytek). Flow data were analyzed using FlowJo software (Treestar).

**Statistical analysis**

All data were analyzed with GraphPad Prism 9 (GraphPad Software). Data are expressed as individual data points $\pm$ SD. For analyses that compared two groups, we used an unpaired Student's *t* test. Statistical significance for more than two genotypes and more than two conditions (*AE* vs. phosphate-buffered saline [PBS] or CFTR modulator(s) vs. vehicle control) was assessed by two-way ANOVA with Bonferroni multiple pairs comparisons test. Values of $P < 0.05$ were considered significant between two groups. For RNAseq analysis, gene counts were normalized using TMM and significant differential expression was determined in genes with FDR-adjusted p value $< 0.01$ and fold change $\pm 1.5$.

**Study approval**

All animal use procedures were approved by the Institutional Animal Care and Use Committee of Vanderbilt University Medical Center. Animals were randomized to different treatment groups. Sample sizes were chosen empirically based on statistical power calculations.

Investigators performing the animal experiments were not blinded to group information. Human PBMCs were obtained from healthy individuals with no prior history of allergy or use of allergy targeting medications after written informed consent and approval by The Vanderbilt University Institutional Review Board.

**Data availability**

FASTQ files containing the raw RNA-seq reads were deposited in the National Center for Biotechnology Information (NCBI) Sequence Reads Archive (SRX2630649[2-7]), with an accompanying BioProject ID (PRJNA1169855). All other data associated with this study are present in the paper or the Supplementary Materials, with data for all data points shown in graphs included in the associated Supporting Data Values file.

**Authors contributions**

Conceptualization: MR, DPC, AEN, CAH, DCN, MHK, RSP. Methodology: MR, DPC, CAH, DCN, MHK, RSP. Investigation: DPC, CMT, MR, JZ, ST, WZ, MA, DY. Visualization: DPC, CMT, MR. Funding acquisition: DPC, RSP. Project administration: JZ, DY. Supervision: DPC, RSP. Writing – original draft: MR, DPC, DCN, MHK, RSP. Writing – review & editing: DPC, CTM, MR, JZ, ST, WZ, MA, DY, AEN, CAH, DCN, MHK, RSP.

# REFERENCES

1. Bojanowski CM, et al. Mucosal Immunity in Cystic Fibrosis. *The Journal of Immunology.* 2021;207(12):2901-12.

2. Skov M, et al. Increased antigen-specific Th-2 response in allergic bronchopulmonary aspergillosis (ABPA) in patients with cystic fibrosis. *Pediatric Pulmonology.* 1999;27(2):74-9.

3. Cook DP, et al. Type 2 inflammation in cystic fibrosis is a predictor of mortality and targeted with CFTR modulator therapy. *Allergy.* 2024.

4. Albon D, et al. Association between Cystic Fibrosis exacerbations, lung function, T2 inflammation and microbiological colonization. *Allergy, Asthma & Clinical Immunology.* 2023;19(1):15.

5. Shanthikumar S, et al. Inflammation in preschool cystic fibrosis is of mixed phenotype, extends beyond the lung and is differentially modified by CFTR modulators. *Thorax.* 2025:thorax-2024-221634.

6. Wojnarowski C, et al. Cytokine expression in bronchial biopsies of cystic fibrosis patients with and without acute exacerbation. *European Respiratory Journal.* 1999;14(5):1136-44.

7. Moss RB, et al. Cytokine dysregulation in activated cystic fibrosis (CF) peripheral lymphocytes. *Clin Exp Immunol.* 2000;120(3):518-25.

8. Knutsen AP, et al. Increased sensitivity to IL-4 in cystic fibrosis patients with allergic bronchopulmonary aspergillosis. *Allergy.* 2004;59(1):81-7.

9. Hartl D, et al. Pulmonary TH2 response in Pseudomonas aeruginosa–infected patients with cystic fibrosis. *Journal of Allergy and Clinical Immunology.* 2006;117(1):204-11.

10. Mueller C, et al. Lack of cystic fibrosis transmembrane conductance regulator in CD3+ lymphocytes leads to aberrant cytokine secretion and hyperinflammatory adaptive immune responses. *Am J Respir Cell Mol Biol.* 2011;44(6):922-9.

11. Elmallah MK, et al. Management of patients with cystic fibrosis and allergic bronchopulmonary aspergillosis using anti-immunoglobulin e therapy (omalizumab). *J Pediatr Pharmacol Ther.* 2012;17(1):88-92.

12. Gothe F, et al. Changes in total IgE levels predict pulmonary outcome in cystic fibrosis related allergic bronchopulmonary aspergillosis. *European Respiratory Journal.* 2016;48(suppl 60):PA1259.

13. Allard JB, et al. Aspergillus fumigatus generates an enhanced Th2-biased immune response in mice with defective cystic fibrosis transmembrane conductance regulator. *J Immunol.* 2006;177(8):5186-94.

14. Litman PM, et al. Serum inflammatory profiles in cystic fibrosis mice with and without Bordetella pseudohinzii infection. *Scientific Reports.* 2021;11(1):17535.

15. Cook DP, et al. Cystic Fibrosis Reprograms Airway Epithelial IL-33 Release and Licenses IL-33 Dependent Inflammation. *Am J Respir Crit Care Med.* 2023.

16. Tiringer K, et al. A Th17- and Th2-skewed cytokine profile in cystic fibrosis lungs represents a potential risk factor for Pseudomonas aeruginosa infection. *Am J Respir Crit Care Med.* 2013;187(6):621-9.

17. Gawenis LR, et al. A BAC Transgene Expressing Human CFTR under Control of Its Regulatory Elements Rescues Cftr Knockout Mice. *Scientific Reports.* 2019;9(1):11828.

18.  Dastoor P, et al. Localization and function of humanized F508del-CFTR in mouse intestine following activation of serum glucocorticoid kinase 1 and Trikafta. *Eur J Pharmacol.* 2024;978:176771.

19.  Cook DP, et al. Cystic Fibrosis Transmembrane Conductance Regulator in Sarcoplasmic Reticulum of Airway Smooth Muscle. Implications for Airway Contractility. *American journal of respiratory and critical care medicine.* 2016;193(4):417-26.

20.  Van Goor F, et al. Rescue of CF airway epithelial cell function in vitro by a CFTR potentiator, VX-770. *Proceedings of the National Academy of Sciences.* 2009;106(44):18825-30.

21.  Yu H, et al. Ivacaftor potentiation of multiple CFTR channels with gating mutations. *Journal of Cystic Fibrosis.* 2012;11(3):237-45.

22.  Hodges CA, et al. Generation of a conditional null allele for Cftr in mice. *Genesis.* 2008;46(10):546-52.

23.  Lee PP, et al. A Critical Role for Dnmt1 and DNA Methylation in T Cell Development, Function, and Survival. *Immunity.* 2001;15(5):763-74.

24.  Klimko N, et al. Mold Allergy in Cystic Fibrosis Patients. *Open Forum Infectious Diseases.* 2016;3(suppl_1).

25.  Wönne R, et al. Bronchial allergy in cystic fibrosis. *Clin Allergy.* 1985;15(5):455-63.

26.  Michorowska S. Ataluren-Promising Therapeutic Premature Termination Codon Readthrough Frontrunner. *Pharmaceuticals (Basel).* 2021;14(8).

27.  Rouillard AD, et al. The harmonizome: a collection of processed datasets gathered to serve and mine knowledge about genes and proteins. *Database (Oxford).* 2016;2016.

28. Seki N, et al. IL-4-induced GATA-3 expression is a time-restricted instruction switch for Th2 cell differentiation. *J Immunol.* 2004;172(10):6158-66.

29. Miller AC, et al. Cystic fibrosis carriers are at increased risk for a wide range of cystic fibrosis-related conditions. *Proceedings of the National Academy of Sciences.* 2020;117(3):1621-7.

30. Knutsen, et al. Asp f I CD4 + TH2-like T-cell lines in allergic bronchopulmonary aspergillosis. *Journal of Allergy and Clinical Immunology.* 1994;94(2, Part 1):215-21.

31. Athari SS. Targeting cell signaling in allergic asthma. *Signal Transduction and Targeted Therapy.* 2019;4(1):45.

32. Shankar A, et al. Modulation of IL-4/IL-13 cytokine signaling in the context of allergic disease. *Journal of Allergy and Clinical Immunology.* 2022;150(2):266-76.

33. Bazett M, et al. Strain-dependent airway hyperresponsiveness and a chromosome 7 locus of elevated lymphocyte numbers in cystic fibrosis transmembrane conductance regulator-deficient mice. *J Immunol.* 2012;188(5):2297-304.

34. Schnell A, et al. Analysis of CFTR mRNA and Protein in Peripheral Blood Mononuclear Cells via Quantitative Real-Time PCR and Western Blot. *Int J Mol Sci.* 2024;25(12).

35. Moss RB, et al. Reduced IL-10 secretion by CD4+ T lymphocytes expressing mutant cystic fibrosis transmembrane conductance regulator (CFTR). *Clin Exp Immunol.* 1996;106(2):374-88.

36. McDonald TV, et al. Human lymphocytes transcribe the cystic fibrosis transmembrane conductance regulator gene and exhibit CF-defective cAMP-regulated chloride current. *Journal of Biological Chemistry.* 1992;267(5):3242-8.

37.     Chen JH, et al. A cAMP-regulated chloride channel in lymphocytes that is affected in cystic fibrosis. *Science.* 1989;243(4891):657-60.

38.     Cheng SH, et al. Defective intracellular transport and processing of CFTR is the molecular basis of most cystic fibrosis. *Cell.* 1990;63(4):827-34.

39.     Younger JM, et al. Sequential quality-control checkpoints triage misfolded cystic fibrosis transmembrane conductance regulator. *Cell.* 2006;126(3):571-82.

40.     Polverino F, et al. CFTR regulates B cell activation and lymphoid follicle development. *Respiratory research.* 2019;20(1):133-.

41.     Galietta LJV, et al. IL-4 Is a Potent Modulator of Ion Transport in the Human Bronchial Epithelium In Vitro1. *The Journal of Immunology.* 2002;168(2):839-45.

42.     Taylor-Cousar JL, et al. CFTR modulator therapy: transforming the landscape of clinical care in cystic fibrosis. *Lancet.* 2023;402(10408):1171-84.

43.     Meng X, et al. Two Small Molecules Restore Stability to a Subpopulation of the Cystic Fibrosis Transmembrane Conductance Regulator with the Predominant Disease-causing Mutation. *J Biol Chem.* 2017;292(9):3706-19.

44.     Csanády L, and Töröcsik B. Cystic fibrosis drug ivacaftor stimulates CFTR channels at picomolar concentrations. *Elife.* 2019;8.

45.     Mehta AM, et al. The impact of CFTR modulator triple therapy on type 2 inflammatory response in patients with cystic fibrosis. *Allergy Asthma Clin Immunol.* 2023;19(1):66.

46.     Bonfield TL, et al. Absence of the cystic fibrosis transmembrane regulator (Cftr) from myeloid-derived cells slows resolution of inflammation and infection. *Journal of leukocyte biology.* 2012;92(5):1111-22.

47.     Bruscia EM, et al. Macrophages directly contribute to the exaggerated inflammatory response in cystic fibrosis transmembrane conductance regulator-/- mice. *American journal of respiratory cell and molecular biology.* 2009;40(3):295-304.

48.     Zhang S, et al. Cystic fibrosis transmembrane conductance regulator (CFTR) modulators have differential effects on cystic fibrosis macrophage function. *Scientific reports.* 2018;8(1):17066-.

49.     Painter RG, et al. CFTR Expression in human neutrophils and the phagolysosomal chlorination defect in cystic fibrosis. *Biochemistry.* 2006;45(34):10260-9.

50.     Ng HP, et al. CFTR targeting during activation of human neutrophils. *J Leukoc Biol.* 2016;100(6):1413-24.

51.     Hector A, et al. Regulatory T-cell impairment in cystic fibrosis patients with chronic pseudomonas infection. *Am J Respir Crit Care Med.* 2015;191(8):914-23.

52.     Yu G, et al. clusterProfiler: an R package for comparing biological themes among gene clusters. *Omics.* 2012;16(5):284-7.

# FIGURES
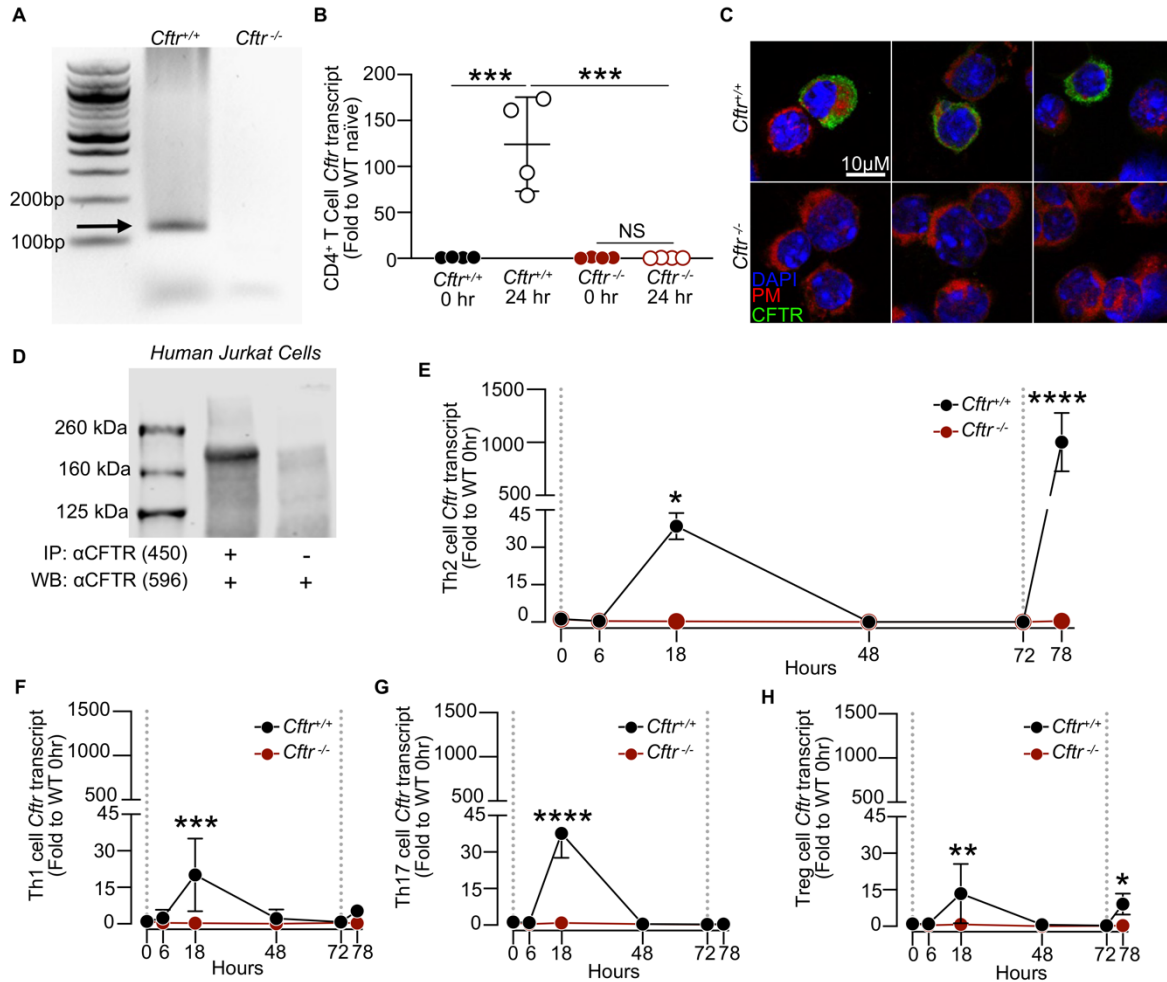


Fig. 1. **CFTR is expressed in CD4$^+$ T cells, induced with CD4$^+$ T cell polarization, and upregulated with Th2 cell reactivation. (A)** Reverse transcriptase polymerase chain reaction for *CFTR* mRNA (predicted size of 125 bp; *arrow*) in *Cftr$^{+/+}$* and *Cftr$^{-/-}$* mouse CD4$^+$ T cells. *Lane 1* is a 100-bp ladder. **(B)** Quantitative PCR (qPCR) analysis of *Cftr* expression in *Cftr$^{+/+}$* and *Cftr$^{-/-}$* mouse CD4$^+$ T cells at 0 and 24 hour following TCR ligation with anti-CD3 and anti-CD28 mAbs ($n = 4$ per genotype and timepoint). **(C)** Immunostaining of CFTR (*green*), plasma membrane lectin (*red*), and nuclei (*blue*) in 24 hour-cultured mouse CD4$^+$ cells (3 different biologic replicates per genotype, *Cftr$^{+/+}$* and *Cftr$^{-/-}$*). *Scale bar* = 10 μm. **(D)** Immunoprecipitated CFTR protein in immortalized human CD4$^+$ T cells (Jurkat) using UNC-450

35

anti-CFTR monoclonal antibody (mAb) for pulldown and UNC-596 anti-CFTR mAb for detection compared with immunoprecipitation isotype control. **(E-H)** qPCR analysis of *Cftr* expression in *Cftr*$^{+/+}$ and *Cftr*$^{-/-}$ cultured mouse CD4$^+$ T cells at 0, 6, 18, 48, 72, and 78 hours in **(E)** Th2, **(F)** Th1, **(G)** Th17, and **(H)** T regulatory (Treg) cells (n = 3 per genotype per timepoint). Dotted lines represent TCR ligation with anti-CD3 (1 µg/ml) and anti-CD28 (0.5 µg/ml) mAbs and 1) anti-IFN-γ (10 µg/ml) and mouse IL-4 (10 ng/ml) for Th2 cells, 2) anti-IL-4 (10 µg/ml) and mouse IL-12 (10 ng/ml) for Th1 cells, and 3) human TGF-β (0.5 ng/ml), mouse IL-23 (10 ng/ml), mouse IL-6 (40 ng/ml), mouse IL-1b (10 ng/ml), anti-IL-4 (10 µg/ml), and anti-IFN-γ (10 µg/ml) for Th17 cells. Tregs were polarized and restimulated with anti-CD3 (1 µg/ml), human IL-2 (100 IU/ml), and recombinant human TGF-β (1ng/ml). Data plotted as mean ± SD. Statistical analysis in (B, E-H) by one-way ANOVA followed by Tukey's honestly significant difference (HSD) post hoc test for multiple comparisons *$P < 0.05$, **$P < 0.01$, ***$P < 0.001$, and ****$P < 0.0001$. NS = not significant.
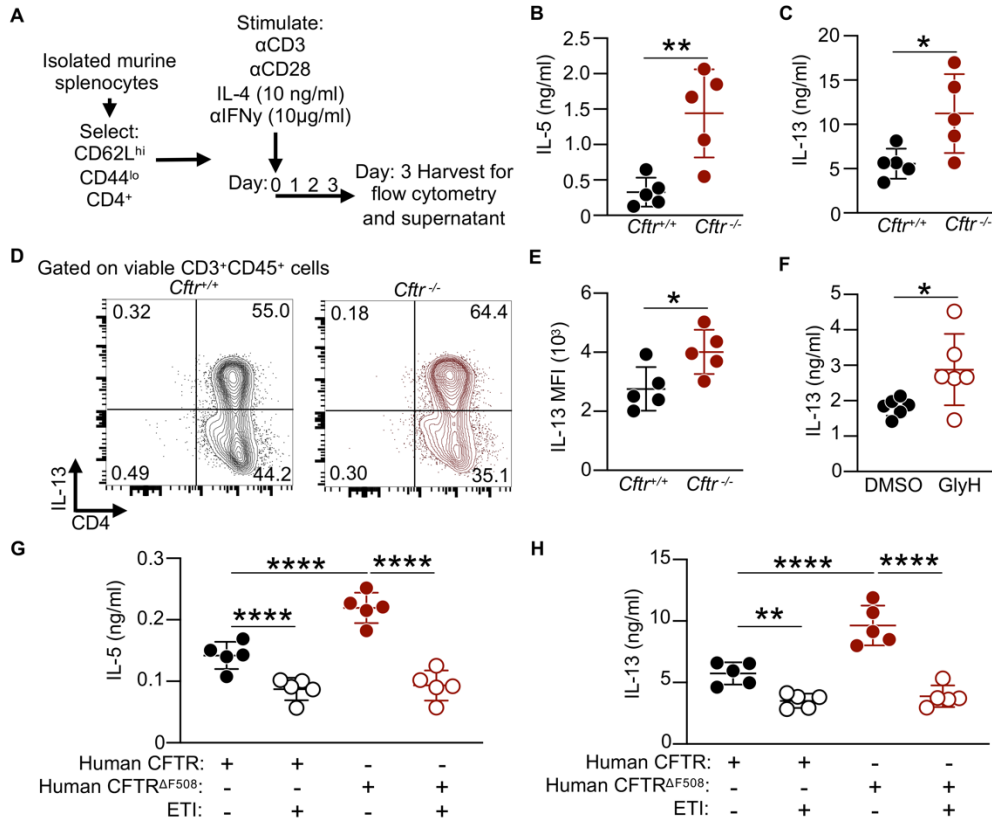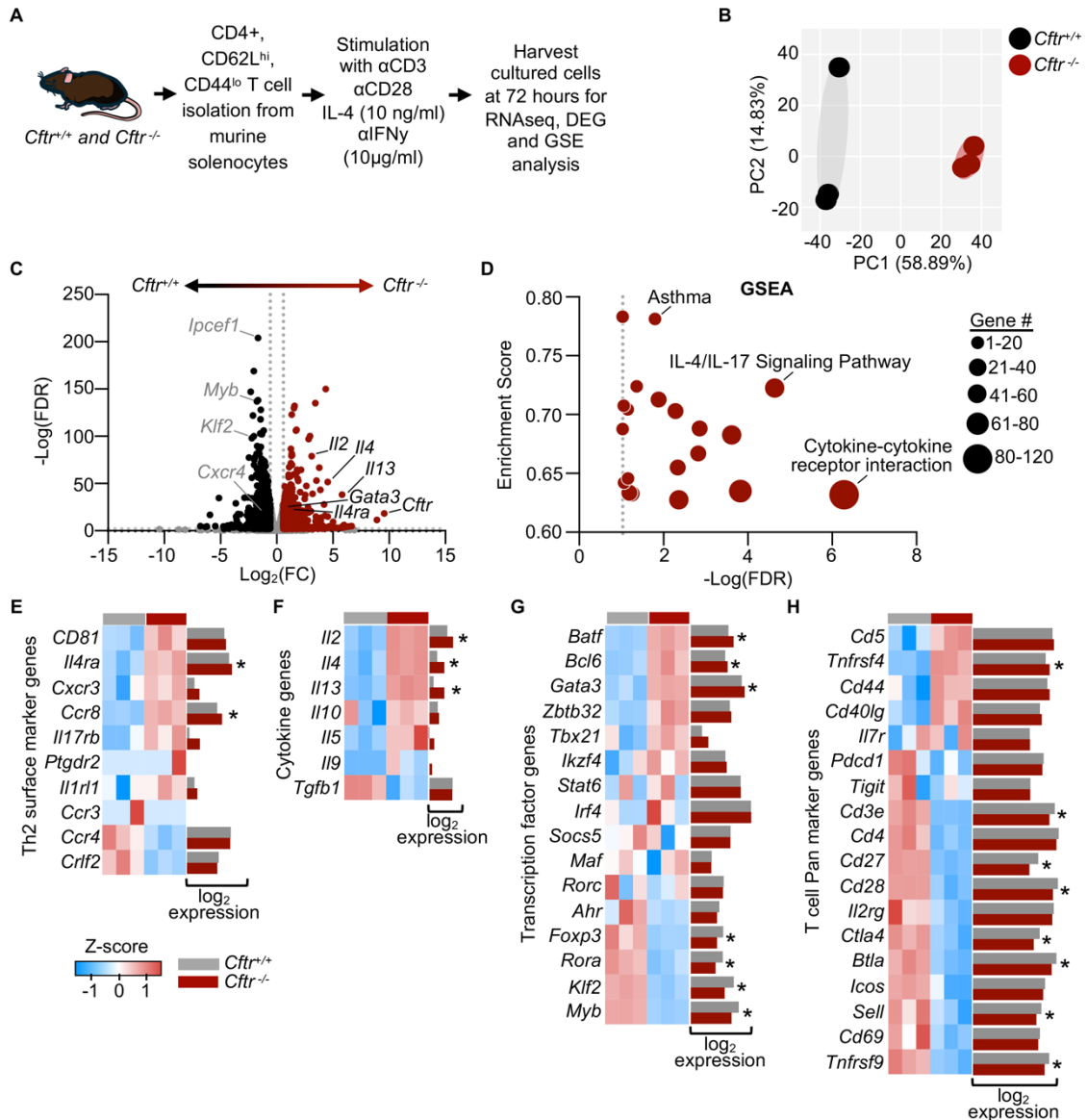
**Fig. 2. Loss of CFTR increases Th2 polarization and effector function. (A)** Schematic diagram showing isolation and stimulation of naïve CD4$^+$ T cells. **(B)** IL-5 and **(C)** IL-13 by ELISA in cellular supernatant from *Cftr*$^{+/+}$ and *Cftr*$^{-/-}$ CD4$^+$ T cells grown in culture stimulated with mouse IL-4 ($n = 5$ mice per genotype). **(D)** Representative gating strategy for IL-13 expression in cultured *Cftr*$^{+/+}$ and *Cftr*$^{-/-}$ CD4$^+$ T cell populations gated on live lymphoid cells. **(E)** IL-13 median fluorescence intensity (MFI) of cultured *Cftr*$^{+/+}$ and *Cftr*$^{-/-}$ CD4$^+$ T cells ($n = 5$ mice per genotype). **(F)** IL-13 by ELISA in cellular supernatant from *Cftr*$^{+/+}$ CD4$^+$ T cells grown in culture with the CFTR inhibitor, GlyH-101, or control vehicle (DMSO) stimulated with mouse IL-4. **(G)** IL-5 and **(H)** IL-13 by ELISA in cellular supernatant from mouse CD4$^+$ T cells expressing either wild-type human CFTR or CFTR$^{\Delta F508}$ grown in culture with Elexacaftor/Tezacaftor/ Ivacaftor (ETI) or DMSO control ($n = 5$ mice per genotype per condition). Data plotted as mean ± SD. Statistical analysis (B-C and E-F) performed using

unpaired student's t test and (G-H) by one-way ANOVA followed by Tukey's honestly significant difference (HSD) post hoc test for multiple comparisons *$P < 0.05$, **$P < 0.01$, and ****$P < 0.0001$.
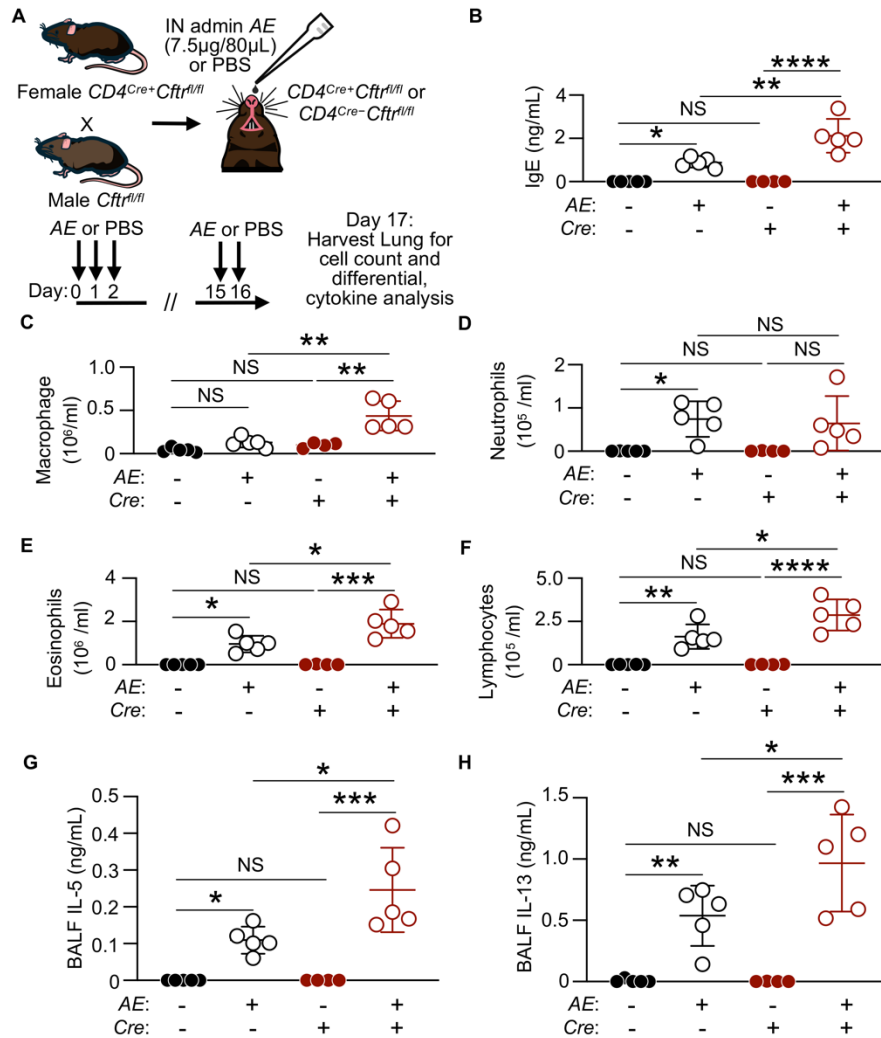
**Fig. 3. CD4$^+$ T cell-specific CFTR deficiency increases *Alternaria* extract (*AE)*-induced allergic inflammation. (A)** Schematic diagram showing adaptive model of intranasal *AE*-induced airway inflammation in *CD4$^{Cre-}$Cftr$^{fl/fl}$* and *CD4$^{Cre+}$Cftr$^{fl/fl}$* mice. **(B)** IgE concentrations by ELISA in serum from treated mice (*n* = 4–5 depending on genotype and condition). The number of **(C)** macrophages, **(D)** neutrophils, **(E)** eosinophils, and **(F)** lymphocytes, in the BALF of phosphate-buffered saline (PBS) or *AE*-challenged mice (*n* = 4–5 per genotype and condition). (**G**) IL-5 and **(H)** IL-13 by ELISA in BAL from *CD4$^{Cre-}$Cftr$^{fl/fl}$* and *CD4$^{Cre+}$Cftr$^{fl/fl}$* mice treated with either *AE* or PBS control (*n* = 4–5 per genotype and condition). Open circles represent *AE* sensitized and challenged mice and closed circles denote PBS control mice. Black circles denote

$CD4^{Cre-}Cftr^{fl/fl}$ and red circles indicate $CD4^{Cre+}Cftr^{fl/fl}$ mice. Statistical analysis in (**B-H)** by one-way ANOVA followed by Tukey's honestly significant difference (HSD) post hoc test for multiple comparisons. *$P < 0.05$, **$P < 0.01$, ***$P < 0.001$, and ****$P < 0.0001$. NS = not significant.

**Fig. 4. Loss of CFTR in Th2 cells increases whole transcriptome type 2 immune specific gene expression. (A)** Schematic diagram showing isolation and polarization of naïve CD4$^+$ T cells to Th2 cells for whole transcriptome analysis. **(B)** PCA plot of gene expression data for three biological replicates used for bulk RNA sequencing of $Cftr^{+/+}$ (black dots) and $Cftr^{-/-}$ (red dots) Th2 cells. **(C)** Volcano plot depicting DESeq2 analysis of differentially expressed genes in $Cftr^{+/+}$ and $Cftr^{-/-}$ Th2 cells. Red dots represent genes expressed at higher levels in $Cftr^{-/-}$ Th2 cells while black dots represent genes with higher expression levels in $Cftr^{+/+}$ Th2 cells. Y-axis

41

denotes $-\log_{10}$ FDR values while X-axis shows $\log_2$ fold change values. Select genes indicated.

**(D)** Advanced bubble plot showing KEGG pathways enriched in *Cftr*$^{-/-}$ Th2 cells. Y-axis denotes enrichment score and $-\log_{10}$ FDR values are shown on X-axis. The size of the bubble represents the number of genes enriched in each pathway. Select pathways indicated. **(E-H)** Heatmaps showing the differential gene expression profile of core Th2 associated genes including **(E)** surface markers, **(F)** cytokines, **(G)** transcription factors, and **(H)** CD4$^+$ pan markers in *Cftr*$^{-/-}$ versus *Cftr*$^{+/+}$ Th2 cells. Normalized $\log_2$ gene expression determined by RNA sequencing shown to the right of each heat map with statistically significant DEGs denoted (*) in *Cftr*$^{+/+}$ (grey bars) and *Cftr*$^{-/-}$ (red bars) Th2 cells. RNA sequencing data was generated in biological triplicates from 3 mice and analyzed via DESeq2. KEGG was used for pathway analysis.
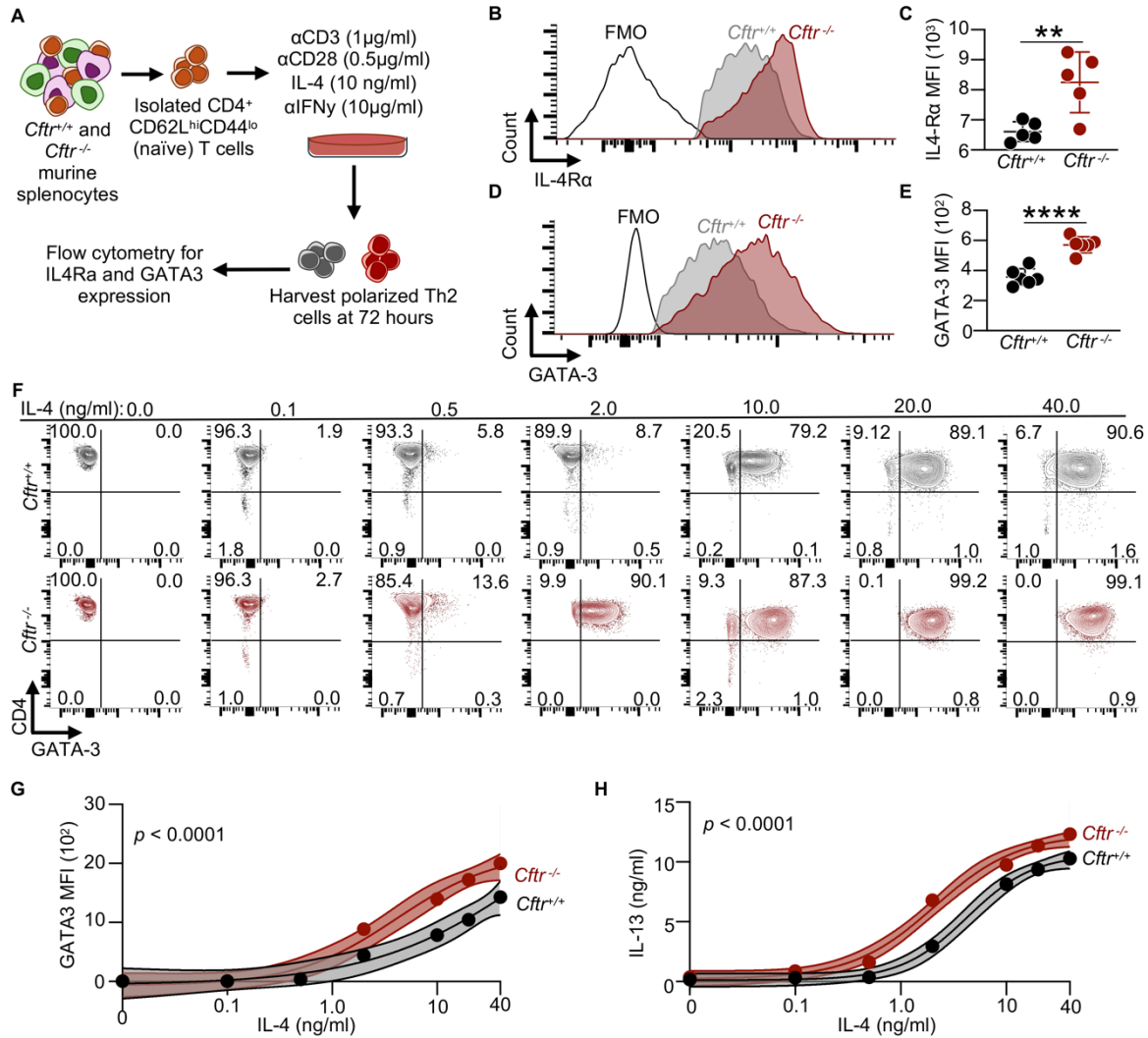
**Fig. 5. CFTR deficiency enhances IL-4 sensitivity and GATA3 expression in Th2 cells. (A)**
Schematic diagram showing isolation and polarization conditions of naïve CD4$^+$ T cells to Th2
cells for IL-4 studies. **(B)** Representative flow cytometry histogram showing the median
fluorescence intensity (MFI) of IL4Rα at 72 hours for *Cftr*$^{+/+}$ and *Cftr*$^{-/-}$ Th2 cells. **(C)** The
quantified MFI of IL4Rα in *Cftr*$^{+/+}$ and *Cftr*$^{-/-}$ Th2 cells at 72 hours (*n* = 5 mice per genotype).
**(D)** Representative flow cytometry histogram showing the MFI of GATA3 at 72 hours for
*Cftr*$^{+/+}$ and *Cftr*$^{-/-}$ Th2 cells. **(E)** The quantified MFI of GATA3 in *Cftr*$^{+/+}$ and *Cftr*$^{-/-}$ Th2 cells at
72 hours (*n* = 5 mice per genotype). **(F)** Representative CD4$^+$ populations showing the MFI of
GATA3 at 72 hours in the presence of increasing doses of polarizing IL-4 (0-40 ng/ml) for

*Cftr*$^{+/+}$ and *Cftr*$^{-/-}$ Th2 cells. (G) GATA3 MFI and **(H)** secreted IL-13 from cellular supernatant in cultured *Cftr*$^{+/+}$ (black) and *Cftr*$^{-/-}$ (red) Th2 cells in the presence of increasing doses of IL-4 (0-40 ng/ml). For (**C and E**), data plotted as mean ± SD. Statistical analysis (C and E) performed using unpaired student's t test and (G and H) four-parameter logistic regression algorithm (sigmoidal curve fit) to fit. For **(G and H)**, data are shown as mean values with the accompanying curve fit (*solid line*), the 95% confidence interval displayed as a band, and mean data points for each genotype and concentration. $**P < 0.01$, and $****P < 0.0001$.
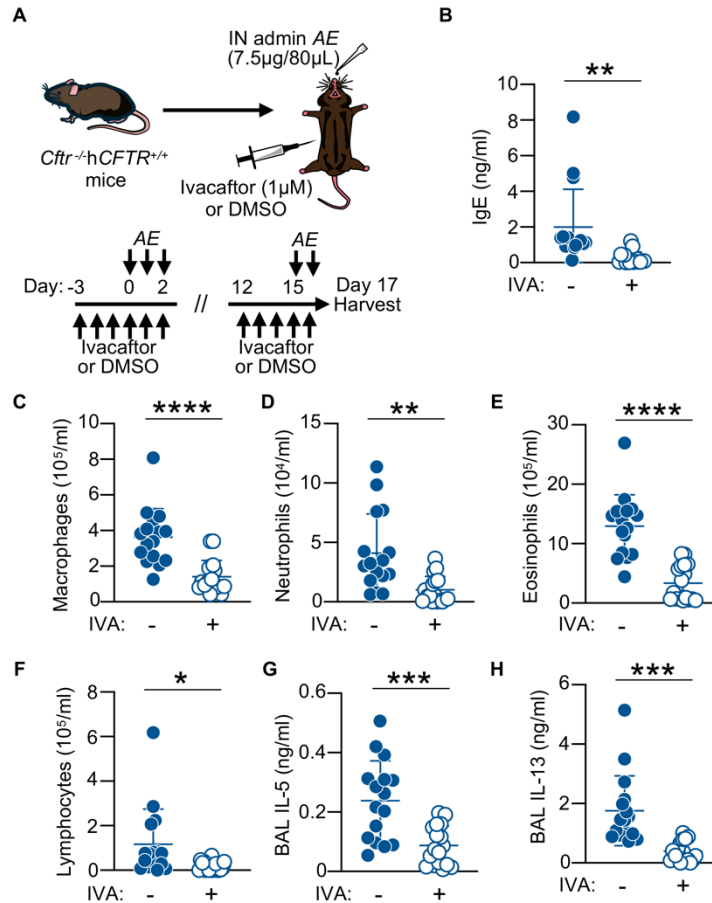
**Fig. 6. Increased CFTR function with ivacaftor decreases allergic inflammation in a humanized CFTR mouse model. (A)** Schematic diagram showing adaptive model of intranasal *AE*-induced inflammation and intraperitoneal ivacaftor (IVA, 1µM) or DMSO administration schedule in *Cftr*⁻/⁻*hCFTR*⁺/⁺ mice. **(B)** IgE concentrations by ELISA in serum from sensitized/challenged mice treated with IVA ($n = 17$) or DMSO ($n = 16$). The number of **(C)** macrophages, **(D)** neutrophils, **(E)** eosinophils, and **(F)** lymphocytes, in the BALF of *AE*-challenged mice treated with either IVA ($n = 17$) or DMSO ($n = 16$). **(G)** IL-5 and **(H)** IL-13 by ELISA in BALF from *AE*-sensitized and challenged mice treated with either IVA ($n = 17$) or DMSO control ($n = 16$). Open circles represent IVA treated mice and closed circles denote DMSO treated control mice. Statistical analysis in (B-H) performed using unpaired student's t test. *$P < 0.05$, **$P < 0.01$, ***$P < 0.001$, and ****$P < 0.0001$. NS = not significant.
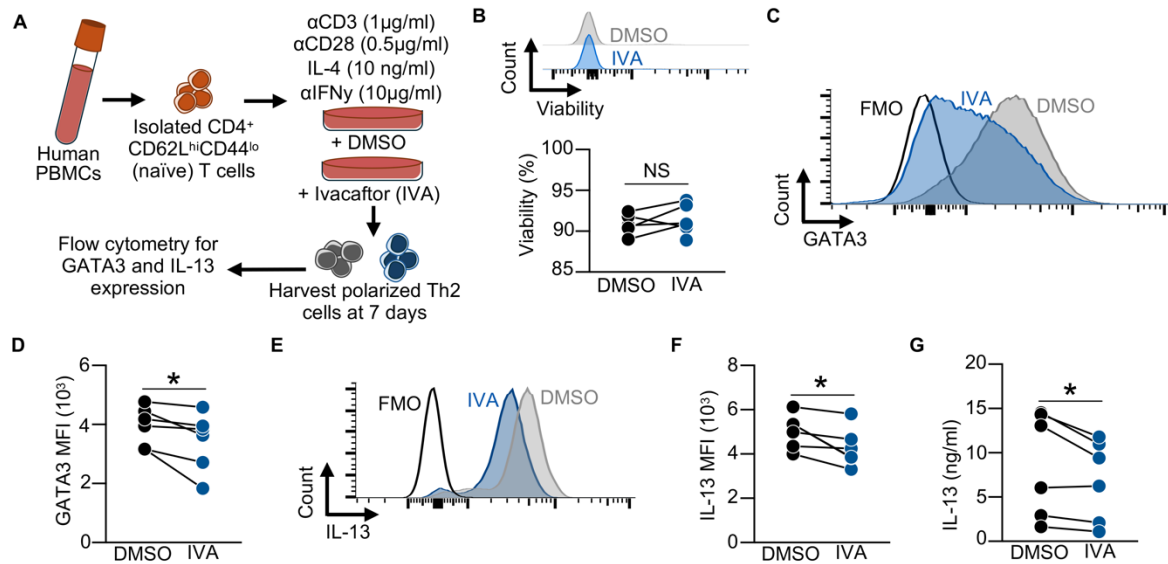
**Figure 7. CFTR potentiation decreases Th2 GATA3 expression and IL-13 production. (A)** Schematic diagram detailing the isolation and Th2 polarization of naïve human CD4$^+$ T cells used for flow cytometry and cytokine analysis. **(B)** Viability of ivacaftor (IVA) or DMSO (control) cultured human Th2 cells at 7 days. **(C)** Representative flow cytometry histogram showing the median fluorescence intensity (MFI) of GATA3 at 7 days for DMSO and IVA treated Th2 cells. **(D)** The quantified MFI of GATA3 in DMSO and IVA treated Th2 cells at 72 hours ($n = 6$ paired human samples). **(E)** Representative flow cytometry histogram showing the median fluorescence intensity (MFI) of IL-13 at 7 days for DMSO and IVA treated Th2 cells. **(F)** The quantified MFI of IL-13 in DMSO and IVA treated Th2 cells at 72 hours ($n = 6$ paired human samples). **(G)** IL-13 by ELISA in cellular supernatant from cultured DMSO and IVA treated Th2 cells. Statistical analysis (B, D, F, and G) performed using paired student's t test. *$P < 0.05$. NS = not significant.